JOURNAL OF RAMAN SPECTROSCOPY
J. Raman Spectrosc. 2008; **39**: 134–140
Published online 26 September 2007 in Wiley InterScience
(www.interscience.wiley.com) DOI: 10.1002/jrs.1824

JRS

Raman scattering from double-walled carbon nanotubes

H. Kuzmany,[1] W. Plank,[1] R. Pfeiffer[1]* and F. Simon[1,2]

[1] Universität Wien, Fakultät für Physik, Strudlhofgasse 4, A-1090 Wien, Austria
[2] Budapest University of Technology and Economics, Institute of Physics, H-1521 Budapest, Hungary

Received 22 June 2007; Accepted 26 July 2007

Raman scattering from double-walled carbon nanotubes is reported with particular emphasis on the response from the radial breathing mode (RBM) of the inner-shell tubes. The unexpected large number of very narrow lines observed is explained by the growth of one and the same inner tube type in different outer tubes in a highly shielded environment. The response of the RBM and of the G-line is used to analyze the transition from peapods to double-walled carbon nanotubes. During the transformation process the Raman response disappears for a short time, indicating the existence of some Raman dark matter. By preparing the starting peapods from heterofullerenes such as $(C_{59}N)_2$ or ^{13}C-substituted fullerenes, hetero-nanotubes can be grown where nitrogen or the ^{13}C atoms are incorporated into the inner tube wall. Copyright © 2007 John Wiley & Sons, Ltd.

KEYWORDS: Raman spectroscopy; double-walled carbon nanotubes; fullerenes; $C_{59}N$

INTRODUCTION

Double-walled carbon nanotubes (DWCNTs) are new members in the family of carbon nanophases. With exactly two walls, they are located between multi-walled carbon nanotubes (MWCNTs) and single-walled carbon nanotubes (SWCNTs) and represent a valuable link between the other two types of tubes which have been very well explored. DWCNTs are particularly attractive for several reasons. Since the inner shell tubes have a typical diameter of 0.7 nm high-curvature effects are well expressed. If the DWCNTs are grown from a peapod precursor material, they exhibit a high degree of perfection, as they are grown in a highly shielded environment. From a technological point of view DWCNTs exhibit higher strength and higher stiffness owing to their shell structure which renders them more appropriate for mechanical problems as, e.g., for tips in scanning probe microscopy or for stability problems in, e.g., field emission applications. Also, the double-wall structure allows for separate inner tube and outer tube functionalization.

DWCNTs can either be prepared from precursor materials in which SWCNTs are filled with carbon-rich molecules such as fullerenes,[1,2] anthracene,[3] or ferrocene[4] and subsequently transformed into DWCNTs by a moderate- or high-temperature reaction, or from chemical vapor deposition reactions with especially tuned deposition parameters.[5]

Raman scattering is a particularly appropriate tool for the study of carbon nanotubes. The strong resonance character of the scattering process allows performing experiments from very small scattering volumes down to individual tubes or small bundles.[6] Owing to the resonance character, not only vibrational but also optical and electronic properties can be probed. This holds in particular for DWCNTs, in which a Raman response from outer tubes and inner tubes can be observed. The sensitivity of some Raman modes to the tube diameter or to tube-wall curvature is another advantage of the Raman technique, which becomes of particular value for the DWCNTs.

Here we review the most important recent results of Raman scattering from DWCNTs with particular attention to some very recent observations on the growth of the inner-shell tubes and possibilities to make heterotubes.

EXPERIMENTAL

SWCNTs were used as purchased from Nanocarblab, Moscow (R-tubes) or as provided by H. Kataura from AIST, Tsukuba (K-tubes) in the form of a buckypaper. In both cases, the typical tube diameter was 1.4 nm. In a buckypaper, the tubes are generally clustered into bundles of several tens individual tubes. For some special experiments and for comparison with the DWCNTs, also HiPco tubes (prepared

*Correspondence to: R. Pfeiffer, Universität Wien, Fakultät für Physik, Strudlhofgasse 4, A-1090 Wien, Austria.
E-mail: rudolf.pfeiffer@univie.ac.at

by high-pressure dissociation of CO) and CoMoCat tubes (prepared from a cobalt molybdenum catalyst) were used. To obtain DWCNTs, the as-provided tubes were first opened by etching with oxygen under ambient conditions at 500 °C and then filled with C_{60} fullerenes, ^{13}C-substituted fullerenes, or $(C_{59}N)_2$ heterofullerenes. Filling was either from the gas phase or from a toluene solution. The peapods so obtained were transformed into DWCNTs by heating in vacuum at 1250 °C for 1 h unless otherwise specified. Since the typical wall-to-wall distance is 0.35 nm the inner tube diameters are of the order of 0.7 nm with a rather narrow diameter distribution.

Raman scattering was performed with a Dilor xy triple spectrometer and excited with a large number of different laser lines with typical laser power of 1–4 mW. Excitation of the spectra was at 80 K unless otherwise indicated. For the high-resolution experiments the spectrometer resolution was 0.5 cm^{-1}.

RAMAN SCATTERING FROM THE RADIAL BREATHING MODE

The radial breathing mode (RBM) is one of the most significant Raman lines in SWCNTs. Since its wavenumber scales as $1/D$, where D is the tube diameter, it has been a valuable tool to characterize the latter. As one can expect from this, DWCNTs should exhibit two signatures in the RBM wavenumber range. As demonstrated in Fig. 1, this is indeed so.

The Raman response from the SWCNTs exhibits one structured line from the various tubes in the buckypaper. In the case of DWCNTs we can see the response from the outer-shell tubes around 180 cm^{-1} almost identical to the response from the SWCNTs, but in addition, the response from the inner-shell tubes around 340 cm^{-1} also appears. This response is unusually strong, has an unexpectedly large number of lines, and line widths down to below 0.5 cm^{-1}.[7] Intensities from the inner shell modes are up to a factor of 2 higher as compared to the response from the outer tubes. This is so in spite of the fact that the overall carbon content in the inner tubes is only about 50% of that in the outer tubes.

The unusually large number of lines can be inferred from a comparison with HiPco tubes which have tubes of similar diameter in the lower part of their diameter distribution. A comparison is provided in Fig. 2.

The upper spectrum is more or less a replica of the high wavenumber part of the RBM response from the DWCNTs in Fig. 1. Roughly speaking, two clusters of lines around 315 and 345 cm^{-1}, respectively, can be seen. As we will demonstrate later, these clusters originate from inner-shell (6,5) and inner-shell (6,4) tubes. The response from the inner-shell tubes is compared to that from the HiPco tubes in the lower spectrum. There is a clear correlation between the two spectra but the higher number of Raman lines in the response from the DWCNTs is obvious.

In order to find the reason for this unexpected increase in the number of Raman lines, one has to measure the resonance Raman profile for each of the lines. This was demonstrated in a general way for normal-resolution Raman spectra by Pfeiffer *et al*. in Ref. 8 Here we demonstrate it for one special set of clusters at high resolution. Figure 3 depicts the high-resolution Raman spectra and the corresponding Raman maps for DWCNTs and for SWCNTs grown from the CoMoCat process.

A section through a constant laser energy in the Raman map yields the Raman spectrum for that laser; a section

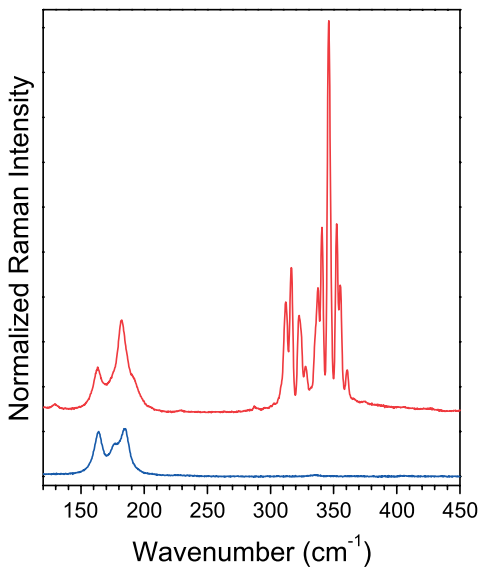

Figure 1. Raman response in the radial breathing mode region of SWCNT (lower spectrum) and of DWCNTs (upper spectrum) for 590 nm laser excitation. This figure is available in colour online at www.interscience.wiley.com/journal/jrs.

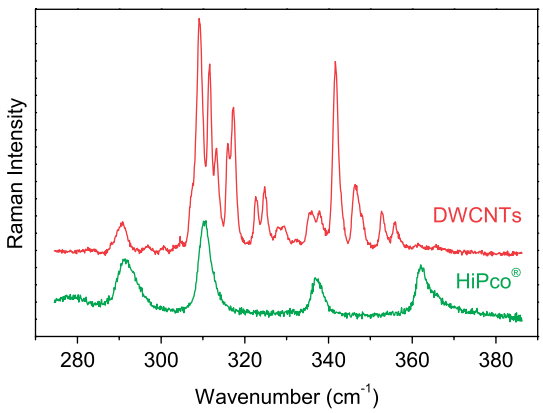

Figure 2. High-resolution Raman response in the radial breathing mode region of DWCNTs (upper spectrum) and SWCNT from a HiPco process (lower spectrum). Laser excitation in both cases was with 568 nm. This figure is available in colour online at www.interscience.wiley.com/journal/jrs.

JRS

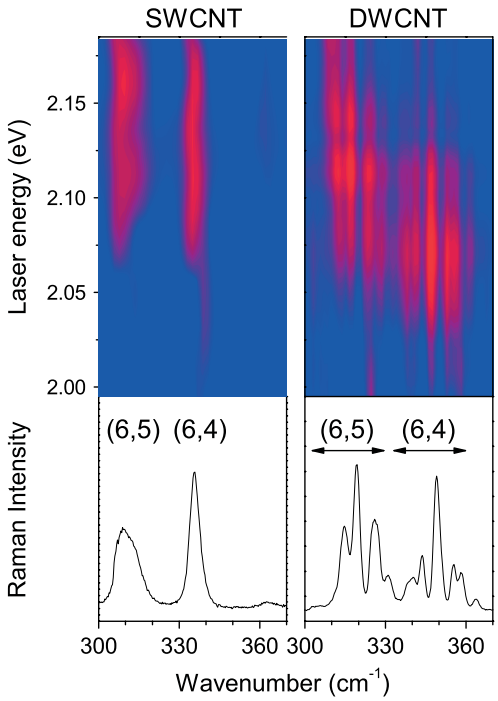

Figure 3. High-resolution Raman spectra from CoMoCat samples (left) and DWCNTs (right) in the RBM regime for excitation with 590 nm (lower part) and Raman map for the same samples in a false-color presentation (upper part).

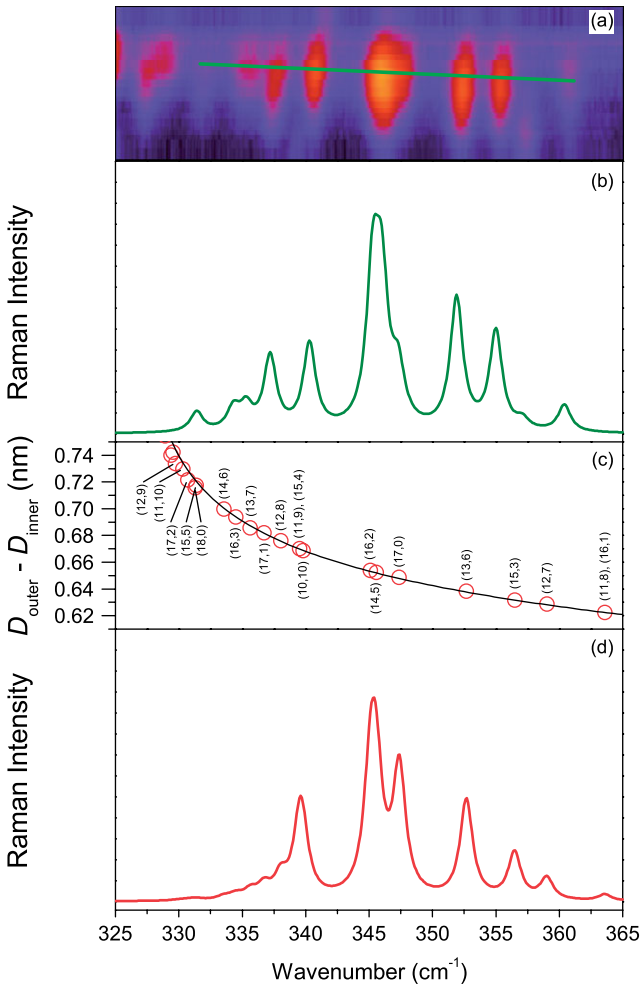

Figure 4. Evaluation of Raman spectra from the RBM in DWCNTs. False-color plot for the cluster of the (6,4) inner tube with a line connecting the positions of the cross-section maxima (a); distribution of inner–outer tube pairs constructed from the false-color plot as described in the text (b); continuum-model calculation of the RBM wavenumber as a function of the diameter difference between the inner and outer tube (c); and distribution of inner–outer tube pairs constructed from the calculations in (c) by dressing the calculated RBM frequencies with Lorentzian lines (d).

through constant Raman shifts yields the scattering cross-section of the particular Raman line. Since all Raman lines have their scattering maximum at about the same laser energy, they correspond to the same inner tube. From a comparison of the maximum in the scattering cross-section with results from HiPco tubes,[9,10] one infers that all Raman lines in one cluster come from the same inner tube. In the case of Fig. 3 these are the tubes (6,5) and (6,4). Obviously these inner tubes can be in various outer tubes, and a different wall-to-wall distance causes a controlled shift of the RBM wavenumber.

In order to obtain more evidence for the above interpretation, the false-color plots were evaluated in a way that allows obtaining the occupation profile for each inner tube in the various outer tubes. This can be done by selecting the positions of each Raman line in the cluster and dressing it with a Lorentzian profile with a peak height corresponding to the maximum observed in the Raman map. The results are depicted in Fig. 4. The top part of the figure represents the false-color plot for the cluster corresponding to the (6,4) tube as taken from an overall Raman map in Ref. 8.

The line connecting the cross-section maxima is slightly inclined by 2 meV/cm^{-1} which reflects the intertube interaction on the electronic transition energies of the selected tube. The line intensities in the 'constructed' spectrum in (b) reflects immediately how often the (6,4) tube is encapsulated in a particular outer tube. Therefore this line pattern allows an immediate comparison to the calculation. From a simple continuum model developed by Pfeiffer *et al.*,[11] the shift of the RBM lines was calculated as a function of the wall-to-wall distance. The result is shown in Fig 4(c). The numbers indicate the outer tube hosting the (6,4) tube. The continuous line is a power-law fit of RBM wavenumbers vs $1/(D_{outer} - D_{inner})$. As expected the tube–tube interaction upshifts the RBM wavenumber with decreasing wall-to-wall distance. Dressing the individual wavenumbers with a Lorentzian line and using line intensities from a Gaussian distribution yields the occupancy of inner tube–outer tube

pairs. There is almost quantitative agreement with the constructed spectrum in Fig. 4(b) and the calculated distribution of the inner tube–outer tube pairs in Fig. 4(d). This strongly supports the model of inner tube–outer tube pairs being responsible for the large number of RBM Raman lines in DWCNTs. Each peak corresponds to a well-defined inner tube–outer tube pair and the particular outer tube can be depicted from Fig. 4(c).

ANALYSIS OF THE GROWTH PROCESS OF INNER SHELL TUBES IN DWCNTS

As described in the introduction, DWCNTs can be grown by several procedures. Whereas growth from a CVD reactor might be the most useful for technological applications, the growth from peapod precursor phases yields the above-described DWCNT species with extremely long life time for the RBM vibrations. The transformation process can be well studied by Raman scattering.

The Raman response from C_{60} peapods has been reported several times.[12] The dominating line, which can also be used for checking the degree of filling, is the pentagonal pinch mode (PPM) of C_{60} located at 1465 cm^{-1} with a small split-off component at 1473 cm^{-1}, when the fullerenes are inside a standard tube. In a series of experiments in which the peapods were exposed to high temperatures in vacuum, we studied the change of the Raman response of these modes for varying exposure times between 0.5 and 300 min at 1250 °C. The result is presented in Fig. 5.

The decay of the pinch mode and the associated mode $H_g(7)$ at 1424 cm^{-1} is rather rapid. After 15 min almost nothing is left from the Raman response. In the right part of the figure the relative line intensity is plotted *vs* exposure time for the two modes. The continuous line is an exponential decay curve for a half-time $T_{1/2} = 2.9$ min.[13]

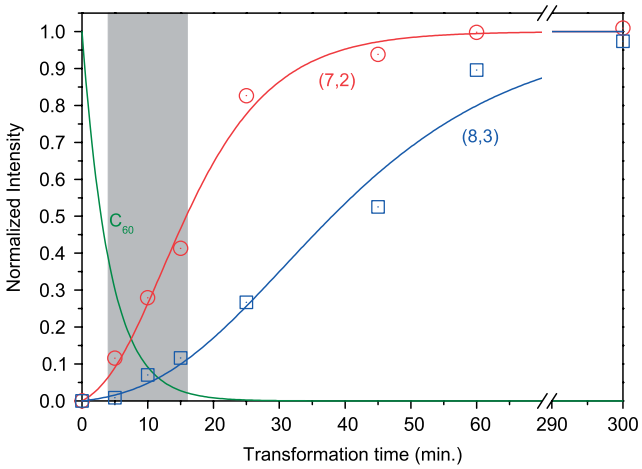

Figure 6. Normalized intensity for the growth of the integrated Raman lines from the tubes (7,2) and (8,3) with diameters $D = 0.64$ and 0.77 nm, respectively. Raman spectra were excited with 676 nm. The red and blue curves are as calculated from an analytical formula given in the text. The green curve represents the decay of the PPM. For the hatched region Raman intensity is missing. This figure is available in colour online at www.interscience.wiley.com/journal/jrs.

Alternatively, one can study the increase of the Raman response from several inner shell tubes. An example is depicted in Fig. 6 for the tubes (7,2) and (8,3). The smaller diameter tube grows more rapidly with a half-time of 16 min. The larger tube (8,3) grows more slowly with a half-time of 38 min.[13] The continuous lines are as calculated from a parameterized Gompertz-like relation

$$I = A\left[e^{B(1-e^{-Ct})} - 1\right] \quad (1)$$

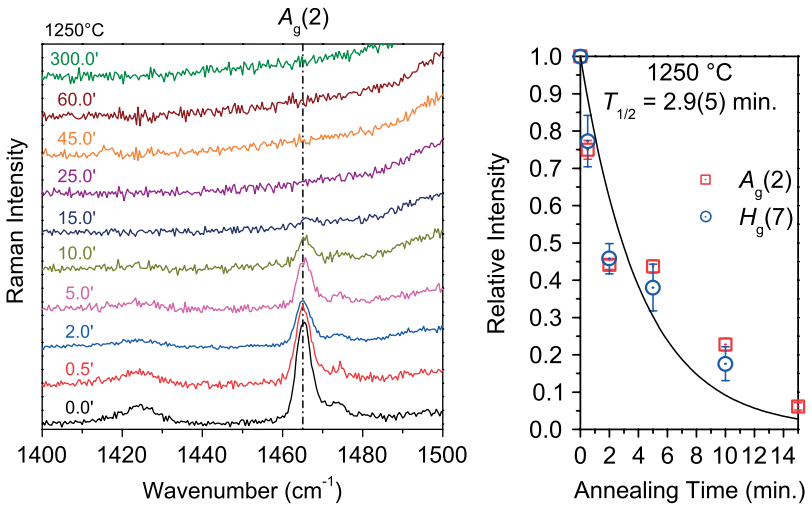

Figure 5. Raman response of the pentagonal pinch mode (PPM) of C_{60} inside SWCNTs after various annealing times at 1250 °C (left) and Raman intensity for various exposure times as normalized to the intensity at zero exposure time for the PPM $A_g(2)$ and for the $H_g(7)$ mode. Laser excitation was at 488 nm. This figure is available in colour online at www.interscience.wiley.com/journal/jrs.

Both growth times for the tubes depicted in Fig. 6 are much longer than the decay time for the fullerenes. The latter is depicted as a green line in the figure for comparison. As a consequence, there must be a transient phase existing between 3 and 15 min, as indicated in the figure by the shaded area. This phase is likely to be a transient state of high disorder and undefined pieces of carbon nanophases which appear during the transformation of the fullerenes to the inner tube. Similar results were observed for other inner-shell tubes. As a general observation, the growth rates of the tubes scale as inverse of their diameter.

The transition from the disordered intermediate state to an ordered state with a high-quality inner shell tube can also be studied by Raman scattering from the G-line. In this case, there is a strong overlap between the response from the outer-shell and inner-shell tubes since the G-line wavenumbers are only weakly dependent on tube diameter. Therefore, to reveal the response from the inner-shell tubes, the response from the outer-shell tubes has to be subtracted. This is done by subtracting the spectrum of the starting peapod material after normalization to the G^+ line (main G-line peak in the spectra). The G-line Raman response obtained in this way is depicted in Fig. 7. The response starts off with very broad lines, which become subsequently narrower with increasing exposure time. The decreasing line width with exposure time is depicted in the main body of the figure.

The rapidly decreasing linewidths are a good indication for increasing order in the system by properly reshaping the tube structures.

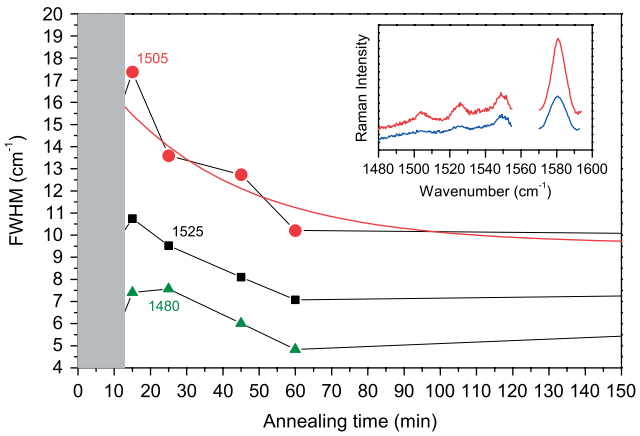

Figure 7. Widths of three different G-line components of the inner-shell tubes as a function of annealing time. The inset depicts the spectra after 15 and 300 min. The response from the outer-shell tubes was subtracted. The peaks are the response of the A_1^{LO} modes of various metallic and semiconducting inner tubes. This figure is available in colour online at www.interscience.wiley.com/journal/jrs.

GROWTH AND ANALYSIS OF HETERO DOUBLE-WALLED CARBON NANOTUBES

The above-described growth of DWCNTs offers another elegant possibility to modify the structure of the inner shell tubes. Two possibilities are evident: filling the tubes with the dimer $(C_{59}N)_2$ (or with a corresponding derivative[14]), or filling the tubes with ^{13}C-enriched fullerenes. Then, upon the transformation of the peas to inner-shell tubes, the hetero atoms might be inserted into the wall of the inner-shell tubes and thus form hetero-DWCNTs.

$(C_{59}N)_2$ is a dimeric heterofullerene in which one carbon on each of the two cages is replaced by a nitrogen atom. Because of the extra electron on the cage, the monomer is a radical and dimerization occurs, therefore, instantly after synthesis. The Raman spectrum of $(C_{59}N)_2$ has been studied previously for several laser excitations.[15] An example is depicted in Fig. 8 in comparison to the response from C_{60}. The $(C_{59}N)_2$ response has a strong resonance for red laser excitation. The dominating line is again the PPM-derived vibration, now at 1462 cm^{-1}. Owing to the loss of almost all symmetry from the originally I_h symmetry in C_{60}, the highly degenerate modes are split up into sharp lines. The origin of these lines was identified in Ref. 15.

$(C_{59}N)_2$ is reasonably stable at room temperature but degrades at high temperatures. Therefore filling of the tubes is preferably done from a toluene solution. In contrast to peapods from C_{60}, unfortunately the response from the encapsulated $(C_{59}N)_2$ is very weak. So far only the signature of the PPM-derived line (arrow in the figure) and a broad

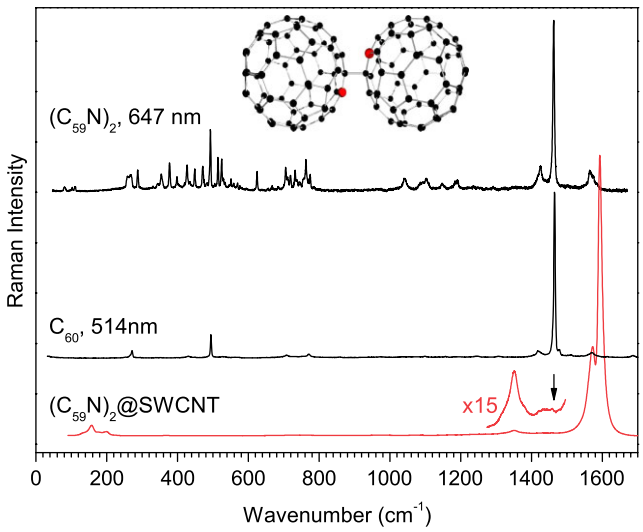

Figure 8. Raman spectra of $(C_{59}N)_2$ and related structures. Raman spectrum of pristine $(C_{59}N)_2$ (top), Raman spectrum of C_{60} for comparison (center), and spectrum from SWCNTs filled with $(C_{59}N)_2$ (bottom). The arrow assigns the response from the filled-in $(C_{59}N)_2$. Laser excitations are as indicated. Inset: molecular structure of $(C_{59}N)_2$. This figure is available in colour online at www.interscience.wiley.com/journal/jrs.

DOI: 10.1002/jrs

feature from the $H_g(7)$-derived line could be detected. Even though these lines provide valuable information on the encapsulated molecule, particularly if compared with the response from encapsulated C_{60} and mixtures of C_{60} with $(C_{59}N)_2$. Such mixtures are interesting since they provide a chance to retain $C_{59}N$ in a monomeric from if the monomers are separated by spin-neutral C_{60} cages.[16] Figure 9 depicts blown-up versions of Raman spectra in the spectral region of the PPM for various species of nanotube peapods.

In the case of C_{60} peapods, we recognize the already well-known response from the $A_g(2)$ mode at 1465 cm^{-1} and from the $H_g(7)$ mode at 1428 cm^{-1}. For filling with $(C_{59}N)_2$, the PPM is downshifted to 1459 cm^{-1} and a broad feature appears around 1438 cm^{-1}. This line probably originates from a split-up and broadened response from $H_g(7)$-derived $(C_{59}N)_2$ modes. Eventually, for the 1 : 1 filled tubes two additional lines appear in the spectrum, one at the position of the PPM of C_{60} and one intermediate between the PPM of $(C_{59}N)_2$ and the $H_g(7)$-derived mode of $(C_{59}N)_2$.

The $(C_{59}N)_2$-filled peapods can be transferred to DWCNTs in the same way as the C_{60} peapods. In this case it can be expected that the N atoms are included into the walls of the inner-shell tubes. Because of the larger mass of the nitrogen atom, this inclusion should result in a downshift of inner-shell vibrational modes. Since this downshift is expected to be rather small, it can best be observed for the overtone of the D-line, located around 2680 cm^{-1}, for the outer-shell tubes and around 2640 cm^{-1} for the inner-shell tubes. For these lines the downshift estimated from the increase of masses is expected to be 4 cm^{-1}. Figure 10 depicts some experimental results.

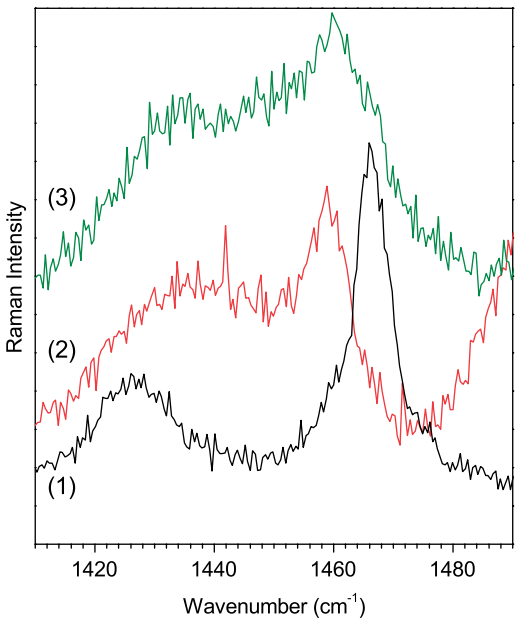

Figure 9. Raman response of various peapod structures in the spectral region of the PPM; tubes filled with C_{60} (1), with $(C_{59}N)_2$ (2), and with a 1 : 1 mixture of C_{60} and $(C_{59}N)_2$ (3). Laser excitation was 488 nm. This figure is available in colour online at www.interscience.wiley.com/journal/jrs.

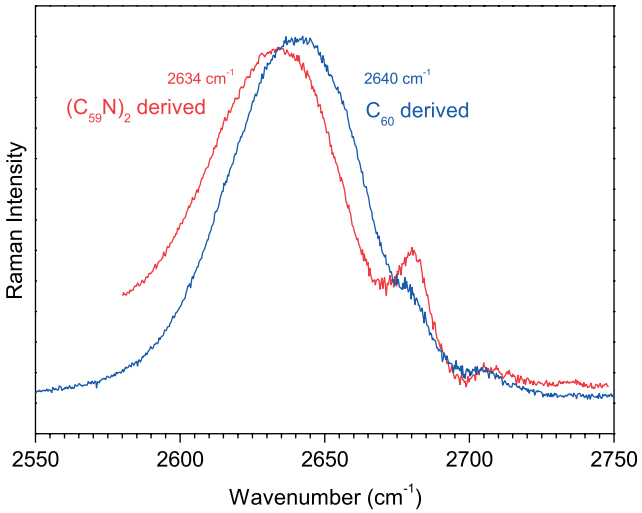

Figure 10. Raman spectra of the D-line overtone (D2-line) from the inner-shell of DWCNTs. The response from the outer-shell tubes was subtracted from the recorded spectra. The lower wavenumber spectrum (red line) is for $(C_{59}N)_2$-derived DWCNTs, and the higher wavenumber spectrum (blue line) is for C_{60}-derived DWCNTs. The indicated numbers are the peak positions. The small features around 2680 cm^{-1} are leftovers from the subtraction process. This figure is available in colour online at www.interscience.wiley.com/journal/jrs.

There is a clear downshift observed for the inner-shell tubes in DWCNTs grown from the $(C_{59}N)_2$ peapods. The experimental value is 6 cm^{-1} and thus very close to the expected downshift from the simple mass formula. It gives strong evidence that the N atoms were fully integrated into the walls of the inner-shell tubes, which renders the latter as strongly doped or hetero-SWCNTs.

Another possibility to obtain hetero-SWCNTs is the filling of the primary tubes with partly (or fully) isotope-substituted fullerenes such as $^{13}C_{60}$. In this case the inner-shell tube will consist partly (or fully) of ^{13}C and provide a different type of hetero-SWCNT. Such substitutions were demonstrated from Raman experiments, which revealed the expected downshift of tube frequencies due to the heavier mass of ^{13}C.[17] ^{13}C-substituted inner-shell tubes are extremely important since ^{13}C has a nuclear spin and therefore allows dedicated NMR experiments.[18]

DISCUSSION

The unusually strong Raman response from the inner-shell tubes is a consequence of an extended life-time of the excited state,[19] which is a factor of 2 higher for the DWCNTs as compared to CoMoCat tubes. Another important consequence of the above analysis is the fact that one can get the Raman response from individually selected tube types

in a well-defined environment, even though the measurements are from an ensemble of tubes. Each line in the cluster represents an ensemble of identical tube types. By extrapolating to very large wall-to-wall distances, the response for the free tube can be obtained. For the case of (6,4) and (6,5), these frequencies are 312 and 276 cm^{-1}, respectively.

The observed increase of time constants with tube diameter supports a model for the growth process in which the fullerenes undergo a fusion initiated by a cyclo-addition reaction. Further reshaping of the growing nanostructure can be performed by Stone–Wales transformations.[20] This interpretation is consistent with the observation of Raman dark matter in the transition region since the highly noncrystalline form of the intermediate phases may provide only a weak resonance and broadened spectra.

In the case of preparing the DWCNTs from $(C_{59}N)_2$ peapods, it remains a challenging question why the response from the PPM- and $H_g(7)$-derived Raman lines are so highly broadened. The difference of the Raman spectra between the $(C_{59}N)_2$-prepared DWCNTs and the DWCNTs prepared from a 1 : 1 mixture between C_{60} and $C_{59}N$ is obvious. It is suggestive to assign this difference to a reaction between the $C_{59}N$ dimer and the C_{60} cages, which would result in a $C_{60}C_{59}N$ heterodimer inside the tubes. The existence of such heterodimers were previously observed from ESR spectra.[16]

The demonstration of implementation of the nitrogen atoms into the inner tube walls is of particular importance. It can be done in a highly controlled manner, as any admixture of pristine C_{60} would continuously reduce the doping concentration. Nitrogen doping adds an extra electron to the conduction band and therefore renders the doped tubes metallic.

The growth of inner-shell tubes from ^{13}C-enriched fullerenes opens a new field in nanotube research as NMR spectroscopy is now ready to enter. Raman scattering will be the crucial technique to determine the eventual ^{13}C concentration from the observed line shifts. It will be particularly helpful to know where the response of the outer-shell tubes and the inner-shell tubes overlap.

In conclusion, we have demonstrated that the Raman response in DWCNTs is able to unravel several unusual properties of the inner-shell tubes extending from the unexpected long phonon life-times to the possibility to functionalize these tubes with various heteroatoms.

Acknowledgements

This work was supported by the Fonds zur Förderung der Wissenschaftlichen Forschung in Österreich, projects P17345 and I83-N20 (ESF-IMPRESS). We acknowledge the supply of $(C_{59}N)_2$ samples by N. Tagmatarchis from the National Hellenic Research Foundation, Greece, and special nanotubes by H. Kataura from AIST, Tsukuba, Japan, and valuable discussions with H. Peterlik in Wien.

REFERENCES

1. Smith BW, Luzzi DE. *Chem. Phys. Lett.* 2000; **321**: 169.
2. Bandow S, Takizawa M, Hirahara K, Yudasaka M, Iijima S. *Chem. Phys. Lett.* 2001; **337**: 48.
3. Kuzmany H, Plank W, Schaman C, Pfeiffer R, Hasi F, Simon F, Rotas G, Pagona G, Tagmatarchis N. *J. Raman Spectrosc.* 2007; **38**: 704.
4. Shiozawa H, Pichler T, Grüneis A, Pfeiffer R, Kuzmany H, Liu Z, Suenaga K, Kataura H. *Catalytic Reaction Inside a Single-wall Carbon Nanotube*, Submitted to Advanced Materials.
5. Endo M, Muramatsu H, Hayashi T, Kim YA, Terrones M, Dresselhaus MS. *Nature* 2005; **433**: 476.
6. Jorio A, Souza Filho AG, Dresselhaus G, Dresselhaus MS, Saito R, Hafner JH, Lieber CM, Matinaga FM, Dantas MSS, Pimenta MA. *Phys. Rev. B* 2001; **63**: 245416.
7. Pfeiffer R, Kuzmany H, Kramberger C, Schaman C, Pichler T, Kataura H, Achiba Y, Kürti J, Zólyomi V. *Phys. Rev. Lett.* 2003; **90**: 225501.
8. Pfeiffer R, Simon F, Kuzmany H, Popov VN. *Phys. Rev. B* 2005; **72**: 161404.
9. Fantini C, Jorio A, Souza M, Strano MS, Dresselhaus MS, Pimenta MA. *Phys. Rev. Lett.* 2004; **93**: 147406.
10. Telg H, Maultzsch J, Reich S, Hennrich F, Thomsen C. *Phys. Rev. Lett.* 2004; **93**: 177401.
11. Pfeiffer R, Kramberger C, Simon F, Kuzmany H, Popov VN, Kataura H. *Eur. Phys. J. B* 2004; **42**: 345.
12. Kuzmany H, Pfeiffer R, Hulman M, Kramberger C. *Philos. Trans. R. Soc. London, Ser. A* 2004; **362**: 2375.
13. Pfeiffer R, Holzweber M, Peterlik H, Kuzmany H, Kataura H. Dynamics of carbon nanotube growth from fullerenes. *Nano Lett.* 2007; **7**: 2428.
14. Simon F, Kuzmany H, Bernardi J, Hauke F, Hirsch A. *Carbon* 2006; **44**: 1958.
15. Kuzmany H, Plank W, Winter J, Dubay O, Tagmatarchis N, Prassides K. *Phys. Rev. B* 1999; **60**: 1005.
16. Simon F, Kuzmany H, Náfrádi B, Fehér T, Forró L, Fülöp F, Jánossy A, Korecz L, Rockenbauer A, Hauke F, Hirsch A. *Phys. Rev. Lett.* 2006; **97**: 136801.
17. Simon F, Kramberger C, Pfeiffer R, Kuzmany H, Zólyomi V, Kürti J, Singer PM, Alloul H. *Phys. Rev. Lett.* 2005; **95**: 017401.
18. Singer PM, Wzietek P, Alloul H, Simon F, Kuzmany H. *Phys. Rev. Lett.* 2005; **95**: 236403.
19. Simon F, Pfeiffer R, Kuzmany H. *Phys. Rev. B* 2006; **74**: 121411.
20. Han S, Yoon M, Berber S, Park N, Osawa E, Ihm J, Tománek D. *Phys. Rev. B* 2004; **70**: 113402.